

Ocean Acidification has Impacted Coral Growth on the Great Barrier Reef

Weifu Guo^{1*}, Rohit Bokade^{1,2}, Anne L. Cohen¹, Nathaniel R. Mollica^{1,3}, Muriel Leung^{1,4},
Russell E. Brainard^{5,6}

¹Department of Geology and Geophysics, Woods Hole Oceanographic Institution, Woods Hole, MA 02543, USA.

²Department of Mechanical and Industrial Engineering, Northeastern University, Boston, MA 02115, USA.

³Massachusetts Institute of Technology-Woods Hole Oceanographic Institution Joint Program in Oceanography, Woods Hole, MA 02543, USA.

⁴Department of Physics and Astronomy, the University of Pennsylvania, Philadelphia, PA 19014, USA.

⁵Pacific Islands Fisheries Science Center, National Oceanic and Atmospheric Administration, Honolulu, HI 96818, USA.

⁶Present address: The Red Sea Development Company, Riyadh, Saudi Arabia.

*Corresponding author: Weifu Guo (wfguo@whoi.edu)

Key Points:

- Numerical model of coral growth isolates the respective impacts of ocean acidification and ocean warming on coral growth.
- Ocean acidification has caused ~13% decline in the skeletal density of massive *Porites* corals on the Great Barrier Reef since 1950.
- OA-induced thinning of coral skeletons reflects enhanced acidification of reef water relative to the surrounding open ocean.

This is the author manuscript accepted for publication and has undergone full peer review but has not been through the copyediting, typesetting, pagination and proofreading process, which may lead to differences between this version and the Version of Record. Please cite this article as doi: [10.1029/2019GL086761](https://doi.org/10.1029/2019GL086761)

1 **Abstract**

2 Ocean acidification (OA) reduces the concentration of seawater carbonate ions that stony corals
3 need to produce their calcium carbonate skeletons, and is considered a significant threat to the
4 functional integrity of coral reef ecosystems. However, detection and attribution of OA impact
5 on corals in nature are confounded by concurrent environmental changes, including ocean
6 warming. Here we use a numerical model to isolate the effects of OA and temperature, and show
7 that OA alone has caused $13\pm 3\%$ decline in the skeletal density of massive *Porites* corals on the
8 Great Barrier Reef since 1950. This OA-induced thinning of coral skeletons, also evident in
9 *Porites* from the South China Sea but not in the central equatorial Pacific, reflects enhanced
10 acidification of reef water relative to the surrounding open ocean. Our finding reinforces
11 concerns that even corals that might survive multiple heatwaves are structurally weakened and
12 increasingly vulnerable to the compounding effects of climate change.

13

14

15

16

17

18

19

20

21 **1. Introduction**

22 About 1/3 of the CO₂ emitted to the atmosphere by human activities has been absorbed
23 by the oceans, driving about 0.1 unit decline in ocean pH and a corresponding ~20% decrease in
24 carbonate ion concentration ([CO₃²⁻]) since the pre-industrial era (e.g., Doney et al., 2009; Feely
25 et al., 2009; Friedlingstein et al., 2019). This process, known as ocean acidification (OA), is
26 expected to continue through this century and beyond, causing another 0.1-0.4 unit pH decline
27 by 2100 and effectively halving the concentration of carbonate ions in seawater relative to the
28 pre-industrial era (e.g., Orr et al., 2005; Doney et al., 2009; Feely et al., 2009). Calcifying
29 organisms, which need carbonate ions to form their skeletons, are most at risk and coral reef
30 ecosystems are expected to be heavily impacted (e.g., Orr et al., 2005; Hoegh-Guldberg et al.,
31 2007). Laboratory experiments that reared corals and other coral reef calcifiers under high CO₂
32 conditions, as well as field studies of naturally low-pH reefs indicate, in general, that decreased
33 rates of calcification and increased rates of dissolution and bioerosion have, and will continue to
34 occur, as the tropical oceans become more acidified over the next few decades (e.g., Pandolfi et
35 al., 2011; Chan and Connolly, 2013).

36 Nevertheless, while measurable ocean acidification of the tropical ocean has been
37 underway for several decades now, detection and attribution of the effects of ocean acidification
38 on reef-building corals have been challenging. Century-long records of coral calcification rates
39 generated from skeletal cores do not show a consistent decline in calcification rates as ocean pH
40 decreased through the 20th century. Rather, in some locations, coral calcification rates sharply
41 decreased, others remained stable, and yet others increased over this time period (e.g., Cooper et
42 al., 2008; De'ath et al., 2009; Cooper et al., 2012; D'Olivo et al., 2013). Even where declines in
43 calcification have been observed, our ability to attribute such changes to ocean acidification is

44 confounded by the fact that ocean warming, sea level rise, changes in surface ocean productivity,
45 as well as many localized anthropogenic disturbances, are co-occurring with ocean acidification
46 and also influence coral growth (e.g., Cooper et al., 2008; De'ath et al., 2009; Lough and Cantin,
47 2014; Pandolfi, 2015).

48 Massive long-lived *Porites* colonies are common on reefs across the Indo-Pacific, and
49 their growth histories span the time period over which ocean acidification has occurred,
50 providing a unique continuous archive of such impacts. The skeletal growth of *Porites* corals
51 occurs in two steps in which the corals initially extend existing skeletal elements to enable
52 upward growth, i.e., extension, followed by thickening of those elements, i.e., densification
53 (Barnes and Lough, 1993). Extension, which is driven primarily by the creation of calcification
54 “centers” or nucleation sites, is under strong biological control (presumably through the organic
55 matrix) and less sensitive to ocean acidification (e.g., Cohen and McConnaughey, 2003;
56 Nothdurft and Webb, 2007; Crook et al., 2013; Fantazzini et al., 2015; Tambutte et al., 2015;
57 Mollica et al., 2018). In contrast, densification, which contributes the bulk of the skeletal mass
58 and serves to reinforce the skeleton against the force of the waves and currents, is strongly
59 sensitive to ocean acidification because crystal formation during this phase is under strong
60 physicochemical control (e.g., Crook et al., 2013; Fantazzini et al., 2015; Tambutte et al., 2015;
61 Mollica et al., 2018; Rippe et al., 2018; Martinez et al., 2019). Here we compile existing and new
62 skeletal growth records of 95 *Porites* corals from the Great Barrier Reef (De'ath et al., 2009),
63 South China Sea (Su et al., 2016) and the central equatorial Pacific Ocean spanning the time
64 period of 1871 to 2014 (Methods, Fig. S1), and use a coral skeletal growth model to isolate the
65 effects of different factors and quantify their respective contributions to the coral growth,
66 particularly to coral skeletal density.

67 2. Methods

68 2.1 *Porites* skeletal growth parameters

69 *Great Barrier Reef (GBR) and South China Sea (SCS, Hainan Island) reefs*: Our analysis
70 employs the annual *Porites* skeletal growth parameters (i.e., extension, density and calcification)
71 reported in previous studies of the Great Barrier Reef (De'ath et al., 2009) and the South China
72 Sea (Hainan Island) reefs (Su et al., 2016). For the Great Barrier Reef, an updated version of the
73 skeletal growth parameters originally reported in (De'ath et al., 2009) is adopted, which excludes
74 the incomplete outmost growth layers (De'ath et al., 2013). Although some other studies also
75 reported *Porites* skeletal growth parameters on the Great Barrier Reef (e.g., D'Oliveo et al., 2013),
76 those data are not available in online repositories and are thus not included in our analysis. To
77 robustly investigate the multi-decadal variations in *Porites* skeletal growth, we focus on the time
78 periods when at least 10 skeletal cores are available for each year and include only cores that
79 have at least 50 years of growth within these selected time periods. Furthermore, we exclude the
80 time periods when independent constraints of environmental parameters (e.g., temperature,
81 Rayner et al., 2003) are not available. Together, these selection criteria result in the inclusion of
82 60 *Porites* cores from 39 reefs over the period of 1871-2000 for the Great Barrier Reef, and 16
83 *Porites* cores from 2 reefs over the period of 1901-2000 for the Hainan Island, South China Sea
84 (Fig. S1). For each core, we calculate the percentage changes in its annual extension, density and
85 calcification relative to the corresponding mean values over 1951-1960, a common period that all
86 cores cover (Fig. S2, Data S1): $x_{i,rel} = \left(x_i / \overline{x_{i,c}} - 1 \right) \cdot 100$, where x_i is the skeletal growth
87 parameter at a given year i and $\overline{x_{i,c}}$ is the mean value of that parameter over the common period
88 for the same core.

89 *Central Equatorial Pacific (CEP) reefs: Porites* skeletal cores were collected from 7 central
90 equatorial Pacific reefs (Jarvis, Kanton, Kingman, Kiritimati, Nikumuroro, Rawaki, Tutuila), and
91 were imaged with a Siemens Volume Zoom Spiral Computerized Tomography scanner. Annual
92 extension rates, skeletal densities and calcification rates were then determined based on these CT
93 images along polyp growth axes (Data S2, DeCarlo et al., 2015; Mollica et al., 2018). Similar to
94 the GBR and South China Sea reef cores, we focus on the time periods when at least 10 skeletal
95 cores are available for each year and include only cores that have at least 10 years of growth
96 within these selected time periods. These lead to the inclusion of 19 *Porites* cores over the period
97 of 1978-2014 in our analysis (Fig. S1). We then calculate, for each core, the percentage changes
98 in its annual extension, density and calcification relative to the corresponding mean values over
99 1998-2007, a common period that all the CEP coral cores cover (see above; Fig. S2, Data S1).

100 **2.2 Predicting *Porites* skeletal density with a skeletal growth model**

101 For each of our selected *Porites* cores, we predict its annual skeletal densities based on a
102 skeletal growth model (Mollica et al., 2018, Text S1) and use them to evaluate and isolate the
103 effects of three main factors that influence *Porites* skeletal density, i.e., extension, temperature,
104 and seawater carbonate chemistry. This skeletal growth model, building on previous studies of
105 *Porites* skeletal growth (Barnes and Lough, 1993; Taylor et al., 1993), explicitly simulates the
106 two distinct phases of *Porites* skeletal growth (i.e., extension and densification) and has
107 quantitatively reproduced the experimentally measured *Porites* skeletal densities from a variety
108 of reef environments (Mollica et al., 2018).

109 For each core, model simulations were conducted under three different conditions: (1)
110 extension as the only forcing, i.e., keeping temperature and seawater carbonate chemistry

111 constant; (2) temperature as the only forcing, i.e., keeping extension and seawater carbonate
112 chemistry constant; (3) extension and temperature combined as the forcing, i.e., keeping
113 seawater carbonate chemistry constant. For the parameters which were kept constant during the
114 model simulations, their values were set as the mean values over the common periods for each
115 core, i.e., 1951-1960 for the Great Barrier Reef and the South China Sea reef cores, and 1998-
116 2007 for the central equatorial Pacific reef cores.

117 For all the model simulations, experimentally measured extension, seawater temperatures
118 from the Hadley Centre Sea Ice and Sea Surface Temperature (HadiSST) v1.1 dataset ($1^\circ \times 1^\circ$,
119 Rayner et al., 2003), and seawater pH and DIC outputs from the Community Earth System
120 Model Biogeochemical historical run (CESM-BGC, Hurrell et al. 2013) were used. HadiSST
121 v1.1 dataset, although relatively coarse in spatial resolution compared to some other temperature
122 datasets (e.g., OISST, Banzon et al., 2016), covers the whole time period of our core records (i.e.,
123 from 1871 to 2014) and has been used extensively in previous reef studies (e.g., De'ath et al.,
124 2009). Similarly, seawater pH and DIC outputs from the CESM-BGC historical run were
125 adopted due to the lack of constraints on past seawater carbonate chemistry in most reefs; but
126 since seawater pH and DIC were kept constant in all our model simulations (see above), their
127 exact values have negligible effects on our results which focus on the relative percentage
128 changes in skeletal density (Mollica et al., 2018). Other parameters in the *Porites* skeletal growth
129 model (e.g., corallite area, tissue thickness) were assumed to be constant over the growth of each
130 coral and set as either the average values reported for *Porites* corals in the region or the
131 optimized values derived from *Porites* corals from multiple tropical reefs (Table S1, Lough and
132 Barnes, 2000; Su et al., 2016; Mollica et al., 2018). We then analyzed these model predicted
133 skeletal densities the same way as the experimentally measured densities, and calculated, for

134 each core, the percentage changes in the model predicted annual densities relative to the
135 corresponding mean of the common periods.

136 **2.3 Constraints on the reef-water pH on the Great Barrier Reef**

137 We compiled existing constraints on the reef-water pH on the Great Barrier Reef based
138 on the boron isotope composition of coral skeletons at six GBR reef sites, including Arlington
139 Reef, Flinders Reef, Pandora Reef, Havannah Island, Rib Reef and Reef 17-065 (Pelejero et al.,
140 2005; Wei et al., 2009; D'Olivo et al., 2015). To robustly investigate the multi-decadal variations
141 in reef-water pH at the Great Barrier Reef, we focused on the time periods when at least 5 pH
142 records were available for each year. This limited our analysis to the period from 1966 to 2000
143 for the Great Barrier Reef (Fig. S3, 7 *Porites* cores in total). To remove the methodological
144 inconsistency in pH estimations among different studies (e.g., regarding the use of boron isotope
145 fractionation factors), we recalculated the seawater pH values based on the coral $\delta^{11}\text{B}$ data
146 reported in each study (Trotter et al., 2011; D'Olivo et al., 2015) using the same physicochemical
147 parameters (Text S2, Data S3, Dickson, 1990; Klochko et al., 2006; Foster et al., 2010). Then,
148 for each $\delta^{11}\text{B}_{\text{coral}}$ record, we calculated changes in its estimated pH_{sw} relative to the
149 corresponding mean over 1976-1985, a common period that all these records cover (Fig. S3,
150 Data S3).

151 There are currently very limited constraints on the reef-water pH for the South China Sea
152 and the central equatorial Pacific reefs (two for the South China Sea reefs, Liu et al., 2014; Wei
153 et al., 2015; none for the central equatorial Pacific reefs), which precludes robust statistical
154 analysis of the temporal trends in reef-water pH for these two regions.

155 **2.4 Determining temporal trends in *Porites* skeletal growth parameters and reef-water pH**

156 We determined the temporal trends in (1) *Porites* skeletal growth parameters (both
157 experimentally measured and model predicted) on the Great Barrier Reef, the South China Sea
158 and the central equatorial Pacific and (2) the reef-water pH records we compiled and recalculated
159 for the Great Barrier Reef, using the Generalized Additive Mixed Models (GAMMs). GAMMs
160 are extensions to the Generalized Linear Mixed Models (GLMMs) and allow for non-linear
161 response (Wood, 2017). Similar methods have been used in previous studies of *Porites* skeletal
162 growth (e.g., De'ath et al., 2009; Cooper et al., 2012; De'ath et al., 2013; Ridd et al., 2013). In
163 each model, year was set as the fixed effect component, while coral colony and reef site as the
164 random effects components. A smoothing spline was applied to the fixed effect variable, with the
165 degree of smoothness (i.e., the degrees of freedom associated with the smoothing function)
166 determined through cross-validation (Cooper et al., 2012). All the models were analyzed using
167 the *lme4* and *mgcv* packages in the R programming software with the REML method (Wood,
168 2011; Bates et al., 2015).

169

170 **3. Results and Discussion**

171 Temporal trends in skeletal growth parameters, determined using generalized additive
172 mixed models (Methods, Wood, 2017), show that *Porites* skeletal density has decreased by
173 ~11% on the Great Barrier Reef from 1871 to 2000 (Fig. 1). This density decline is most
174 significant between 1980 and 2000 reaching ~3% per decade, compared to ~0.5% per decade
175 from 1871 to 1980. Declines in skeletal density are also evident in *Porites* colonies in the South
176 China Sea and in the central equatorial Pacific, ranging from ~20% over 1901-2000 to ~7% over
177 1978-2014, respectively (Fig. S4).

178 These density declines, although consistent with the negative impacts expected from OA,
179 cannot be attributed exclusively to OA, because factors including skeletal extension (E) and
180 seawater temperature also influence coral skeletal density (Fig. 2). Specifically, as extension
181 increases, density will decrease, even if ocean pH does not change, because the less time a
182 skeletal element resides within the coral tissue layer (i.e., at higher extension rate) the less it can
183 be thickened, and vice versa (Barnes and Lough, 1993; Taylor et al., 1993; Mollica et al., 2018).
184 Conversely, skeletal density is expected to increase as seawater temperature increases, because
185 calcium carbonate precipitates faster at higher temperatures (Burton and Walter, 1987; Mollica et
186 al., 2018). Note, other environmental factors such as nutrients and water quality can also affect
187 coral growth mostly through their influences on extension (e.g., Dustan, 1975; Huston, 1985;
188 Tomascik and Sander, 1985; Lough and Cooper, 2011; Al-Rousan, 2012), and are thus implicitly
189 included in our analysis as well (Fig. 2).

190 Indeed, at all three study sites, the density declines observed in the *Porites* corals over
191 time were accompanied by increases in skeletal extension, ranging from ~9% at the Great Barrier
192 Reef to ~30% in the South China Sea, and by temperature variations up to 1.5°C (Fig. 1, 3, S4-
193 S5). We estimated the contribution of these extension and temperature changes to the observed
194 density declines, using a skeletal growth model that explicitly simulates the two-step skeletal
195 growth of *Porites* corals and links the coral calcifying fluid chemistry with external seawater
196 conditions (Methods, Mollica et al., 2018). The model predicts that skeletal extension acting
197 alone would have caused a modest decline in skeletal density of ~4% on the Great Barrier Reef
198 over the time period from 1871 to 2000 (Fig. 3a). Conversely, variations in water temperature
199 alone, especially the increase post-1950, would have caused a ~6% increase in skeletal density
200 over the same time period (Fig. 3b). Together, skeletal extension and ocean warming are

201 expected to lead to oscillations of *Porites* skeletal density between -2% and 2% during 1871-
202 2000, not the decrease in density as observed (Fig. 3c).

203 Ocean acidification, skeletal extension and temperature are the main influences of the
204 skeletal density of *Porites* corals (Fig. 2, Mollica et al., 2018). Previous model simulations,
205 explicitly considering these three factors, have quantitatively reproduced the experimentally
206 measured *Porites* skeletal densities from a variety of reef environments (Mollica et al., 2018).
207 Thus, having constrained the effects of temperature and extension, we can assess the impact of
208 OA on *Porites* density (DD_{OA}) by subtracting the model predicted density changes induced by
209 extension and temperature variations ($DD_{E+T, modeled}$) from the measured density changes (
210 $DD_{measured}$):

$$211 \quad DD_{OA} = DD_{measured} - DD_{E+T, modeled} \quad (1)$$

212 Figure 3c shows that the OA-driven changes in the skeletal density of *Porites* corals on the Great
213 Barrier Reef since 1871. OA-driven changes are small, fluctuating between 2 and -2%, until
214 1950, after which a rapid $\sim 13 \pm 3\%$ (95% confidence interval) decline in density is observed from
215 1950 to 2000. The timing of the OA effect is consistent with the accelerated decline in the ocean
216 pH post-1950. However, the magnitude of the ocean pH decrease post-1950 is too small to
217 explain the dramatic decline in skeletal density on the GBR. In fact, the skeletal growth model
218 predicts a density change of $\sim 1\%$ given a 0.06 change in seawater pH alone.

219 This discrepancy is explained by the enhanced acidification of reef-water on the GBR
220 relative to the open ocean (Fig. 4a, Methods, Pelejero et al., 2005; Wei et al., 2009; D'Olivo et al.,
221 2015). In particular, boron isotope analysis of *Porites* skeleton shows that reef-water pH on the

222 Arlington Reef (mid-shelf, northern GBR) has decreased by ~0.2 unit since the 1940s (Methods,
223 Wei et al., 2009), which is about 2.5-fold larger than the decrease in open ocean pH over the
224 same time period (i.e., ~0.06 unit). This enhanced acidification of reef-water has also been
225 observed at inshore reefs in the GBR and at other coral reefs around the globe, where reef-water
226 pCO₂ has increased 2.5~3.5-fold faster than the open ocean over the past 20-30 years potentially
227 as a result of increased inputs of terrestrial nutrient and organic matter (Fig. 4a, Cyronak et al.,
228 2014; Uthicke et al., 2014).

229 Our model does predict some high-frequency density variability that is not replicated in
230 the measured data, especially around 1940. This variability is driven by the temperature input to
231 the model. It is likely that well-documented uncertainties in the historical temperature data-
232 products during this time period (e.g., Chelton and Risien, 2016) confound our estimation of the
233 temperature effects on *Porites* density and caused the ~4% decline in density around 1940 that
234 we currently attribute to OA. Efforts to increase the accuracy of the historical temperature
235 records (e.g., Chan et al., 2019) will improve our estimates of the OA impact on coral skeletal
236 growth. Overall however, the model-predicted effects of extension and temperature on skeletal
237 density are in good agreement with the independently measured density changes (Fig. 3a-b) and
238 our results indicate strong impacts of OA on GBR corals post-1950.

239 Analysis of *Porites* growth records from Hainan Island, South China Sea indicate that
240 here too, OA has caused ~7±3% (95% confidence interval) decline in *Porites* skeletal density
241 from 1901 to 2000, with the most significant decline also starting around 1950 (Fig. 4b, S5, Text
242 S4). The similar timing of the estimated OA impacts on the GBR and the South China Sea corals
243 occurs despite the dramatically different bulk skeletal growth records at these two regions (Fig.
244 S4), and is consistent with the similar evolution of ocean pH around the GBR and the South

245 China Sea (Fig. 4b). In contrast, analysis of central equatorial Pacific reef corals suggests that
246 OA has not yet had a significant influence on *Porites* growth in the region (Fig. 4b, S5, Text S4).
247 This is likely because these reefs are bathed in open-ocean seawaters and have thus experienced
248 relatively modest decreases in their reef-water pH to date.

249 Our study presents strong evidence that 20th century ocean acidification, exacerbated by
250 reef biogeochemical processes, has had measurable effects on the growth of a key reef-building
251 coral across the Great Barrier Reef and in the South China Sea, and will likely accelerate as
252 ocean acidification progresses over the next several decades. While it is difficult to directly
253 extrapolate our estimated OA impact to any specific reef due to the variability of reef-water pH
254 among and within different reefs (e.g., Gagliano et al., 2010; Uthicke et al., 2014; D'Olivo et al.,
255 2015; Mongin et al., 2016), we expect broadly similar magnitudes of OA impact worldwide
256 because enhanced acidification of reef water pH similar to the GBR has been observed in many
257 coral reefs around the globe (Fig. 4a, Cyronak et al., 2014).

258 Declines in coral skeletal density increase the susceptibility of coral skeletons to
259 bioerosion, dissolution and storm damage (e.g., Madin et al., 2012; Wisshak et al., 2012; Crook
260 et al., 2013; DeCarlo et al., 2015; Fantazzini et al., 2015), and suggest structurally weaker and
261 more vulnerable coral reefs in the 21st century. In particular, the strength of coral skeleton
262 decreases exponentially with decreasing skeletal density, e.g., about 60% reduction of
263 compressive strength for a 13% density decline (Chamberlain, 1978; Scott and Risk, 1988;
264 Madin, 2004; Madin et al., 2008), making the coral skeletons increasingly susceptible to storm
265 damage. This, together with the deleterious influences of other global and local environmental
266 stressors (e.g., ocean warming, sea level rise, pollution), poses severe challenges for the health
267 and survival of coral reef ecosystems and their exceptional biodiversity. Better understanding of

268 the controls on the reef-water pH and coral calcification mechanisms will enable more accurate
269 projections of OA impacts on coral reef ecosystems and thus the developments of potential
270 mitigation strategies.

271

272

273 **Acknowledgements**

274 The data generated in this study are being archived at the NOAA National Centers for
275 Environmental Information-Paleoclimatology Data repository, i.e., the World Data Service for
276 Paleoclimatology. For review purposes, a copy of the data has been provided in the Supporting
277 Information (Data S1-S3).

278

279

280

281

282

283

284

285

286

287 **References**

- 288 Al-Rousan, S. (2012) Skeletal extension rate of the reef building coral *Porites* species from
289 Aqaba and their environmental variables. *Nat. Sci.* 4, 731-739.
- 290 Banzon, V., Smith, T.M., Chin, T.M., Liu, C.Y. and Hankins, W. (2016) A long-term record of
291 blended satellite and in situ sea-surface temperature for climate monitoring, modeling and
292 environmental studies. *Earth System Science Data* 8, 165-176.
293 <https://doi.org/10.5194/essd-8-165-2016>
- 294 Barnes, D.J. and Lough, J.M. (1993) On the nature and causes of density banding in massive
295 coral skeletons. *J. Exp. Mar. Biol. Ecol.* 167, 91-108. [https://doi.org/10.1016/0022-0981\(93\)90186-r](https://doi.org/10.1016/0022-0981(93)90186-r)
- 296
- 297 Bates, D., Maechler, M., Bolker, B. and Walker, S. (2015) Fitting linear mixed-effects models
298 using lme4. *J. Stat. Softw.* 67, 1-48.
- 299 Burton, E.A. and Walter, L.M. (1987) Relative precipitation rates of aragonite and mg calcite
300 from seawater: temperature or carbonate ion control? *Geology* 15, 111-114.
301 [https://doi.org/10.1130/0091-7613\(1987\)15%3C111:rproaa%3E2.0.co;2](https://doi.org/10.1130/0091-7613(1987)15%3C111:rproaa%3E2.0.co;2)
- 302 Chamberlain, J.A. (1978) Mechanical-properties of coral skeleton - compressive strength and its
303 adaptive significance. *Paleobiology* 4, 419-435.
- 304 Chan, D., Kent, E.C., Berry, D.I. and Huybers, P. (2019) Correcting datasets leads to more
305 homogeneous early-twentieth-century sea surface warming. *Nature* 571, 393-397.
306 <https://doi.org/10.1038/s41586-019-1349-2>
- 307 Chan, N.C.S. and Connolly, S.R. (2013) Sensitivity of coral calcification to ocean acidification: a
308 meta-analysis. *Glob. Change Biol.* 19, 282-290. <https://doi.org/10.1111/gcb.12011>
- 309 Chelton, D.B. and Risien, C.M. (2016) Zonal and Meridional Discontinuities and Other Issues
310 with the HadISST1.1 Dataset (Technical report).
311 <https://ir.library.oregonstate.edu/concern/defaults/kw52j9632>.
- 312 Cohen, A.L. and McConnaughey, T.A. (2003) Geochemical perspectives on coral mineralization.
313 *Rev. Mineral. Geochem.* 54, 151-187. <https://doi.org/10.2113/0540151>
- 314 Cooper, T.F., De 'Ath, G., Fabricius, K.E. and Lough, J.M. (2008) Declining coral calcification
315 in massive *Porites* in two nearshore regions of the northern Great Barrier Reef. *Glob.*
316 *Change Biol.* 14, 529-538. <https://doi.org/10.1111/j.1365-2486.2007.01520.x>
- 317 Cooper, T.F., O'Leary, R.A. and Lough, J.M. (2012) Growth of western Australian corals in the
318 Anthropocene. *Science* 335, 593-596. <https://doi.org/10.1126/science.1214570>
- 319 Crook, E.D., Cohen, A.L., Rebolledo-Vieyra, M., Hernandez, L. and Paytan, A. (2013) Reduced
320 calcification and lack of acclimatization by coral colonies growing in areas of persistent
321 natural acidification. *Proc. Nat. Acad. Sci. U.S.A.* 110, 11044-11049.
322 <https://doi.org/10.1073/pnas.1301589110>
- 323 Cyronak, T., Schulz, K.G., Santos, I.R. and Eyre, B.D. (2014) Enhanced acidification of global
324 coral reefs driven by regional biogeochemical feedbacks. *Geophys. Res. Lett.* 41, 5538-
325 5546. <https://doi.org/10.1002/2014gl060849>
- 326 D'Olivo, J.P., McCulloch, M.T., Eggins, S.M. and Trotter, J. (2015) Coral records of reef-water
327 pH across the central Great Barrier Reef, Australia: assessing the influence of river runoff
328 on inshore reefs. *Biogeosciences* 12, 1223-1236. <https://doi.org/10.5194/bg-12-1223-2015>
- 329

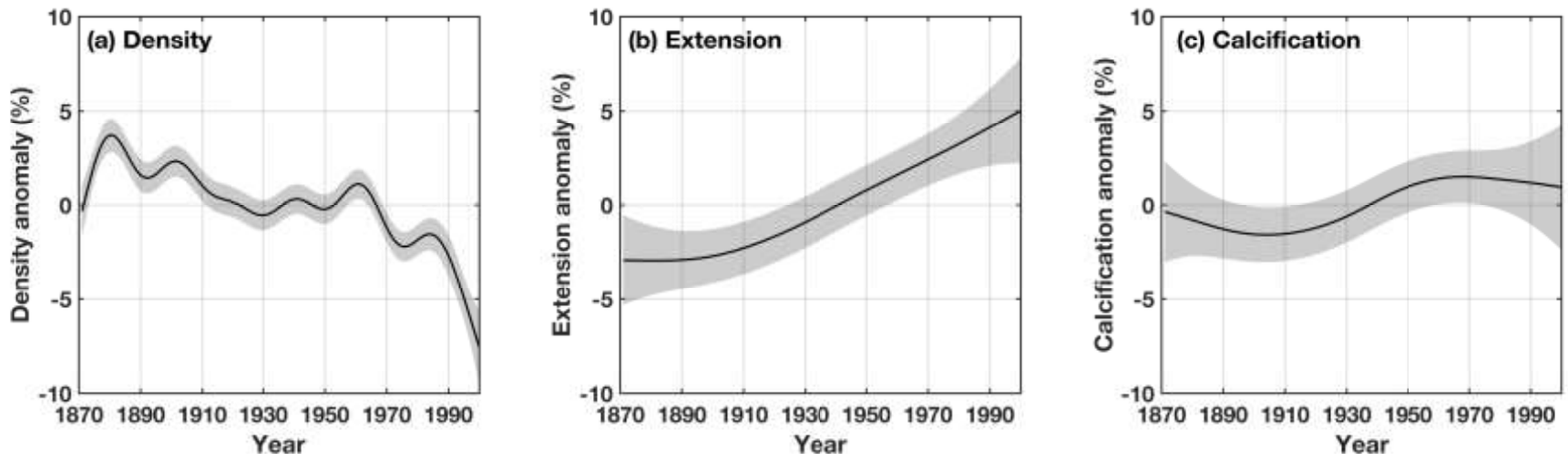
- 330 D'Olivo, J.P., McCulloch, M.T. and Judd, K. (2013) Long-term records of coral calcification
331 across the central Great Barrier Reef: assessing the impacts of river runoff and climate
332 change. *Coral Reefs* 32, 999-1012. <https://doi.org/10.1007/s00338-013-1071-8>
- 333 De'ath, G., Fabricius, K. and Lough, J. (2013) Yes - Coral calcification rates have decreased in
334 the last twenty-five years! *Mar. Geol.* 346, 400-402.
335 <https://doi.org/10.1016/j.margeo.2013.09.008>
- 336 De'ath, G., Lough, J.M. and Fabricius, K.E. (2009) Declining coral calcification on the Great
337 Barrier Reef. *Science* 323, 116-119. <https://doi.org/10.1126/science.1165283>
- 338 DeCarlo, T.M., Cohen, A.L., Barkley, H.C., Cobban, Q., Young, C., Shamberger, K.E., Brainard,
339 R.E. and Golbuu, Y. (2015) Coral macrobioerosion is accelerated by ocean acidification
340 and nutrients. *Geology* 43, 7-10. <https://doi.org/10.1130/g36147.1>
- 341 Dickson, A.G. (1990) Thermodynamics of the dissociation of boric-acid in synthetic seawater
342 from 273.15 K to 318.15 K. *Deep Sea Res. A* 37, 755-766.
343 [https://doi.org/10.1016/0198-0149\(90\)90004-f](https://doi.org/10.1016/0198-0149(90)90004-f)
- 344 Doney, S.C., Fabry, V.J., Feely, R.A. and Kleypas, J.A. (2009) Ocean acidification: The other
345 CO₂ problem. *Annu. Rev. Mar. Sci.* 1, 169-192.
346 <https://doi.org/10.1146/annurev.marine.010908.163834>
- 347 Dustan, P. (1975) Growth and form in reef-building coral *Montastrea annularis*. *Mar. Biol.* 33,
348 101-107. <https://doi.org/10.1007/bf00390714>
- 349 Fantazzini, P., Mengoli, S., Pasquini, L., Bortolotti, V., Brizi, L., Mariani, M., Di Giosia, M.,
350 Fermani, S., Capaccioni, B., Caroselli, E., Prada, F., Zaccanti, F., Levy, O., Dubinsky, Z.,
351 Kaandorp, J.A., Konglerd, P., Hammel, J.U., Dauphin, Y., Cuif, J.P., Weaver, J.C.,
352 Fabricius, K.E., Wagermaier, W., Fratzi, P., Falini, G. and Goffredo, S. (2015) Gains and
353 losses of coral skeletal porosity changes with ocean acidification acclimation. *Nat.*
354 *Commun.* 6, 7785. <https://doi.org/10.1038/ncomms8785>
- 355 Feely, R.A., Doney, S.C. and Cooley, S.R. (2009) Ocean Acidification: Present conditions and
356 future changes in a high-CO₂ world. *Oceanography* 22, 36-47.
357 <https://doi.org/10.5670/oceanog.2009.95>
- 358 Foster, G.L., Pogge von Strandmann, P.A.E. and Rae, J.W.B. (2010) Boron and magnesium
359 isotopic composition of seawater. *Geochem. Geophys. Geosyst.* 11.
360 <https://doi.org/10.1029/2010gc003201>
- 361 Friedlingstein, P., Jones, M.W., O'Sullivan, M., Andrew, R.M., Hauck, J., Peters, G.P., Peters,
362 W., Pongratz, J., Sitch, S., Le Quere, C., Bakker, D.C.E., Canadell, J.G., Ciais, P.,
363 Jackson, R.B., Anthoni, P., Barbero, L., Bastos, A., Bastrikov, V., Becker, M., Bopp, L.,
364 Buitenhuis, E., Chandra, N., Chevallier, F., Chini, L.P., Currie, K.I., Feely, R.A., Gehlen,
365 M., Gilfillan, D., Gkritzalis, T., Goll, D.S., Gruber, N., Gutekunst, S., Harris, I., Haverd,
366 V., Houghton, R.A., Hurtt, G., Ilyina, T., Jain, A.K., Joetzjer, E., Kaplan, J.O., Kato, E.,
367 Goldewijk, K.K., Korsbakken, J.I., Landschutzer, P., Lauvset, S.K., Lefevre, N., Lenton,
368 A., Lienert, S., Lombardozzi, D., Marland, G., McGuire, P.C., Melton, J.R., Metzl, N.,
369 Munro, D.R., Nabel, J., Nakaoka, S.I., Neill, C., Omar, A.M., Ono, T., Peregón, A.,
370 Pierrot, D., Poulter, B., Rehder, G., Resplandy, L., Robertson, E., Rodenbeck, C.,
371 Seferian, R., Schwinger, J., Smith, N., Tans, P.P., Tian, H.Q., Tilbrook, B., Tubiello, F.N.,
372 van der Werf, G.R., Wiltshire, A.J. and Zaehle, S. (2019) Global Carbon Budget 2019.
373 *Earth System Science Data* 11, 1783-1838. [https://doi.org/10.5194/essd-11-1783-](https://doi.org/10.5194/essd-11-1783-2019)
374 [2019](https://doi.org/10.5194/essd-11-1783-2019)

- 375 Gagliano, M., McCormick, M.I., Moore, J.A. and Depczynski, M. (2010) The basics of
376 acidification: baseline variability of pH on Australian coral reefs. *Mar. Biol.* 157, 1849-
377 1856. <https://doi.org/10.1007/s00227-010-1456-y>
- 378 Guo, W. (2019) Seawater temperature and buffering capacity modulate coral calcifying pH. *Sci.*
379 *Rep.* 9, 1189. <https://doi.org/10.1038/s41598-018-36817-y>
- 380 Hoegh-Guldberg, O., Mumby, P.J., Hooten, A.J., Steneck, R.S., Greenfield, P., Gomez, E.,
381 Harvell, C.D., Sale, P.F., Edwards, A.J., Caldeira, K., Knowlton, N., Eakin, C.M.,
382 Iglesias-Prieto, R., Muthiga, N., Bradbury, R.H., Dubi, A. and Hatziolos, M.E. (2007)
383 Coral reefs under rapid climate change and ocean acidification. *Science* 318, 1737-1742.
384 <https://doi.org/10.1126/science.1152509>
- 385 Hurrell, J.W., Holland, M.M., Gent, P.R., Ghan, S., Kay, J.E., Kushner, P.J., Lamarque, J.F.,
386 Large, W.G., Lawrence, D., Lindsay, K., Lipscomb, W.H., Long, M.C., Mahowald, N.,
387 Marsh, D.R., Neale, R.B., Rasch, P., Vavrus, S., Vertenstein, M., Bader, D., Collins,
388 W.D., Hack, J.J., Kiehl, J. and Marshall, S. (2013) The Community Earth System Model
389 A Framework for Collaborative Research. *Bull. Am. Meteorol. Soc.* 94, 1339-1360.
390 <https://doi.org/10.1175/bams-d-12-00121.1>
- 391 Huston, M. (1985) Variation in coral growth-rates with depth at Discovery Bay, Jamaica. *Coral*
392 *Reefs* 4, 19-25. <https://doi.org/10.1007/bf00302200>
- 393 Klochko, K., Kaufman, A.J., Yao, W.S., Byrne, R.H. and Tossell, J.A. (2006) Experimental
394 measurement of boron isotope fractionation in seawater. *Earth Planet. Sci. Lett.* 248,
395 276-285. <https://doi.org/10.1016/j.epsl.2006.05.034>
- 396 Liu, Y., Peng, Z.C., Zhou, R.J., Song, S.H., Liu, W.G., You, C.F., Lin, Y.P., Yu, K.F., Wu, C.C.,
397 Wei, G.J., Xie, L.H., Burr, G.S. and Shen, C.C. (2014) Acceleration of modern
398 acidification in the South China Sea driven by anthropogenic CO₂. *Sci. Rep.* 4, 5148.
399 <https://doi.org/10.1038/srep05148>
- 400 Lough, J.M. and Barnes, D.J. (2000) Environmental controls on growth of the massive coral
401 *Porites*. *J. Exp. Mar. Biol. Ecol.* 245, 225-243. [https://doi.org/10.1016/s0022-0981\(99\)00168-9](https://doi.org/10.1016/s0022-0981(99)00168-9)
- 402 Lough, J.M. and Cantin, N.E. (2014) Perspectives on massive coral growth rates in a changing
403 ocean. *Biol. Bull.* 226, 187-202. <https://doi.org/10.1086/BBLv226n3p187>
- 404 Lough, J.M. and Cooper, T.F. (2011) New insights from coral growth band studies in an era of
405 rapid environmental change. *Earth Sci. Rev.* 108, 170-184.
406 <https://doi.org/10.1016/j.earscirev.2011.07.001>
- 407 Madin, J.S. (2004) A mechanistic approach to understanding and predicting hydrodynamic
408 disturbance on coral reefs., Department of Marine Biology and Aquaculture. James Cook
409 University.
- 410 Madin, J.S., Hughes, T.P. and Connolly, S.R. (2012) Calcification, storm damage and population
411 resilience of tabular corals under climate change. *Plos One* 7, e46637.
412 <https://doi.org/10.1371/journal.pone.0046637>
- 413 Madin, J.S., O'Donnell, M.J. and Connolly, S.R. (2008) Climate-mediated mechanical changes to
414 post-disturbance coral assemblages. *Biology Letters* 4, 490-493.
415 <https://doi.org/10.1098/rsbl.2008.0249>
- 416 Martinez, A., Crook, E.D., Barshis, D.J., Potts, D.C., Rebolledo-Vieyra, M., Hernandez, L. and
417 Paytan, A. (2019) Species-specific calcification response of Caribbean corals after 2-year
418 transplantation to a low aragonite saturation submarine spring. *Proceedings of the Royal*
419 *Society B-Biological Sciences* 286. <https://doi.org/10.1098/rspb.2019.0572>
- 420

- 421 McCulloch, M., Falter, J., Trotter, J. and Montagna, P. (2012) Coral resilience to ocean
422 acidification and global warming through pH up-regulation. *Nat. Clim. Change* 2, 623-
423 633. <https://doi.org/10.1038/nclimate1473>
- 424 McCulloch, M.T., D'Olivo, J.P., Falter, J., Holcomb, M. and Trotter, J.A. (2017) Coral
425 calcification in a changing World and the interactive dynamics of pH and DIC
426 upregulation. *Nat. Commun.* 8, 15686. <https://doi.org/10.1038/ncomms15686>
- 427 Mollica, N.R., Guo, W.F., Cohen, A.L., Huang, K.F., Foster, G.L., Donald, H.K. and Solow, A.R.
428 (2018) Ocean acidification affects coral growth by reducing skeletal density. *Proc. Nat.*
429 *Acad. Sci. U.S.A.* 115, 1754-1759. <https://doi.org/10.1073/pnas.1712806115>
- 430 Mongin, M., Baird, M.E., Tilbrook, B., Matear, R.J., Lenton, A., Herzfeld, M., Wild-Allen, K.,
431 Skerratt, J., Margvelashvili, N., Robson, B.J., Duarte, C.M., Gustafsson, M.S.M., Ralph,
432 P.J. and Steven, A.D.L. (2016) The exposure of the Great Barrier Reef to ocean
433 acidification. *Nat. Commun.* 7, 10732. <https://doi.org/10.1038/ncomms10732>
- 434 Nothdurft, L.D. and Webb, G.E. (2007) Microstructure of common reef-building coral genera
435 *Acropora*, *Pocillopora*, *Goniastrea* and *Porites*: constraints on spatial resolution in
436 geochemical sampling. *Facies* 53, 1-26. <https://doi.org/10.1007/s10347-006-0090-0>
- 437 Orr, J.C., Fabry, V.J., Aumont, O., Bopp, L., Doney, S.C., Feely, R.A., Gnanadesikan, A.,
438 Gruber, N., Ishida, A., Joos, F., Key, R.M., Lindsay, K., Maier-Reimer, E., Matear, R.,
439 Monfray, P., Mouchet, A., Najjar, R.G., Plattner, G.K., Rodgers, K.B., Sabine, C.L.,
440 Sarmiento, J.L., Schlitzer, R., Slater, R.D., Totterdell, I.J., Weirig, M.F., Yamanaka, Y.
441 and Yool, A. (2005) Anthropogenic ocean acidification over the twenty-first century and
442 its impact on calcifying organisms. *Nature* 437, 681-686.
443 <https://doi.org/10.1038/nature04095>
- 444 Pandolfi, J.M. (2015) Incorporating uncertainty in predicting the future response of coral reefs to
445 climate change. *Annu. Rev. Ecol. Evol. Syst.* 46, 281-303.
446 <https://doi.org/10.1146/annurev-ecolsys-120213-091811>
- 447 Pandolfi, J.M., Connolly, S.R., Marshall, D.J. and Cohen, A.L. (2011) Projecting coral reef
448 futures under global warming and ocean acidification. *Science* 333, 418-422.
449 <https://doi.org/10.1126/science.1204794>
- 450 Pelejero, C., Calvo, E., McCulloch, M.T., Marshall, J.F., Gagan, M.K., Lough, J.M. and Opdyke,
451 B.N. (2005) Preindustrial to modern interdecadal variability in coral reef pH. *Science* 309,
452 2204-2207. <https://doi.org/10.1126/science.1113692>
- 453 Rayner, N.A., Parker, D.E., Horton, E.B., Folland, C.K., Alexander, L.V., Rowell, D.P., Kent,
454 E.C. and Kaplan, A. (2003) Global analyses of sea surface temperature, sea ice, and night
455 marine air temperature since the late nineteenth century. *J. Geophys. Res.-Atmos.* 108.
456 <https://doi.org/10.1029/2002jd002670>
- 457 Ridd, P.V., da Silva, E.T. and Stieglitz, T. (2013) Have coral calcification rates slowed in the last
458 twenty years? *Mar. Geol.* 346, 392-399.
459 <https://doi.org/10.1016/j.margeo.2013.09.002>
- 460 Rippe, J.P., Baumann, J.H., De Leener, D.N., Aichelman, H.E., Friedlander, E.B., Davies, S.W.
461 and Castillo, K.D. (2018) Corals sustain growth but not skeletal density across the Florida
462 Keys Reef Tract despite ongoing warming. *Glob. Change Biol.* 24, 5205-5217.
463 <https://doi.org/10.1111/gcb.14422>
- 464 Scott, P.J.B. and Risk, M.J. (1988) The effect of *lithophaga* (bivalvia, mytilidae) boreholes on
465 the strength of the coral *Porites lobata*. *Coral Reefs* 7, 145-151.
466 <https://doi.org/10.1007/bf00300974>

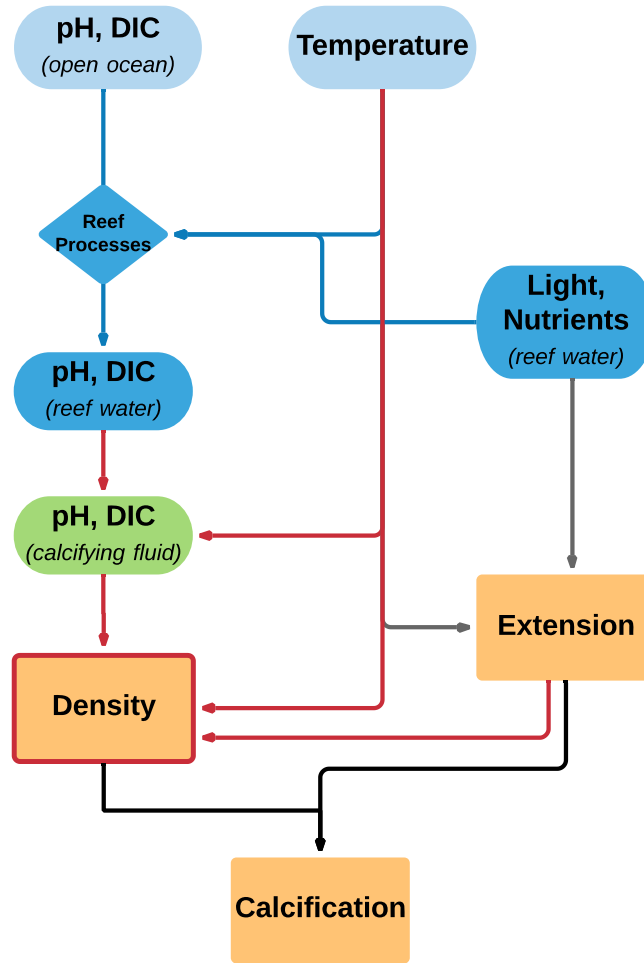
- 467 Su, R.X., Lough, J.M. and Sun, D.H. (2016) Variations in massive *Porites* growth rates at
468 Hainan Island, northern South China Sea. *Mar. Ecol. Prog. Ser.* 546, 47-60.
469 <https://doi.org/10.3354/meps11654>
- 470 Tambutte, E., Venn, A.A., Holcomb, M., Segonds, N., Techer, N., Zoccola, D., Allemand, D.
471 and Tambutte, S. (2015) Morphological plasticity of the coral skeleton under CO₂-driven
472 seawater acidification. *Nat. Commun.* 6, 7368. <https://doi.org/10.1038/ncomms8368>
- 473 Taylor, R.B., Barnes, D.J. and Lough, J.M. (1993) Simple-models of density band formation in
474 massive corals. *J. Exp. Mar. Biol. Ecol.* 167, 109-125. [https://doi.org/10.1016/0022-
475 0981\(93\)90187-s](https://doi.org/10.1016/0022-0981(93)90187-s)
- 476 Tomascik, T. and Sander, F. (1985) Effects of eutrophication on reef-building corals .I. Growth
477 rate of the reef-building coral *Montastrea annularis*. *Mar. Biol.* 87, 143-155.
478 <https://doi.org/10.1007/bf00539422>
- 479 Trotter, J., Montagna, P., McCulloch, M., Silenzi, S., Reynaud, S., Mortimer, G., Martin, S.,
480 Ferrier-Pagès, C., Gattuso, J.-P. and Rodolfo-Metalpa, R. (2011) Quantifying the pH
481 'vital effect' in the temperate zooxanthellate coral *Cladocora caespitosa*: Validation of the
482 boron seawater pH proxy. *Earth Planet. Sci. Lett.* 303, 163-173.
483 <https://doi.org/10.1016/j.epsl.2011.01.030>
- 484 Uthicke, S., Furnas, M. and Lonborg, C. (2014) Coral reefs on the edge? Carbon chemistry on
485 inshore reefs of the Great Barrier Reef. *Plos One* 9, e109092.
486 <https://doi.org/10.1371/journal.pone.0109092>
- 487 Wei, G.J., McCulloch, M.T., Mortimer, G., Deng, W.F. and Xie, L.H. (2009) Evidence for ocean
488 acidification in the Great Barrier Reef of Australia. *Geochim. Cosmochim. Acta* 73, 2332-
489 2346. <https://doi.org/10.1016/j.gca.2009.02.009>
- 490 Wei, G.J., Wang, Z.B., Ke, T., Liu, Y., Deng, W.F., Chen, X.F., Xu, J.F., Zeng, T. and Xie, L.H.
491 (2015) Decadal variability in seawater pH in the West Pacific: Evidence from coral $\delta^{11}\text{B}$
492 records. *J. Geophys. Res.-Oceans* 120, 7166-7181.
493 <https://doi.org/10.1002/2015jc011066>
- 494 Wisshak, M., Schonberg, C.H.L., Form, A. and Freiwald, A. (2012) Ocean acidification
495 accelerates reef bioerosion. *Plos One* 7.
496 <https://doi.org/10.1371/journal.pone.0045124>
- 497 Wood, S.N. (2011) Fast stable restricted maximum likelihood and marginal likelihood estimation
498 of semiparametric generalized linear models. *J. R. Stat. Soc. Ser. B* 73, 3-36.
- 499 Wood, S.N. (2017) Generalized Additive Models: An Introduction with R (2nd edition).
500 Chapman and Hall/CRC.

501



502
503
504
505
506
507
508
509
510
511

Fig. 1. Partial-effects plots showing changes in *Porites* skeletal parameters at the Great Barrier Reef from 1871 to 2000: (a) density, (b) extension, and (c) calcification. The temporal trends were derived from 60 long (≥ 50 years) *Porites* skeletal cores from 39 reefs across the Great Barrier Reef (Fig. S1, Methods, Text S3, De'ath et al., 2009), and are expressed as the anomalies relative to the corresponding mean values over 1951-1960, a common period that all cores cover. The gray bands indicate 95% confidence intervals for the predicted value for any given year.



512

513

514 **Fig. 2. Relations between open ocean and reef water carbonate chemistry and their**

515 **influences on *Porites* coral skeletal growth.** *Porites* skeletal density is directly affected by the

516 carbonate chemistry of its calcifying fluid, which in turn is influenced by reef-seawater

517 chemistry (Mollica et al., 2018; Guo, 2019, Text S1). This makes *Porites* skeletal density most

518 sensitive to ocean acidification. Besides seawater chemistry, *Porites* skeletal density is also

519 directly affected by seawater temperature and the rate of skeletal extension (Mollica et al., 2018),

520 while other environmental factors (e.g., light condition, nutrient levels) affect *Porites* skeletal

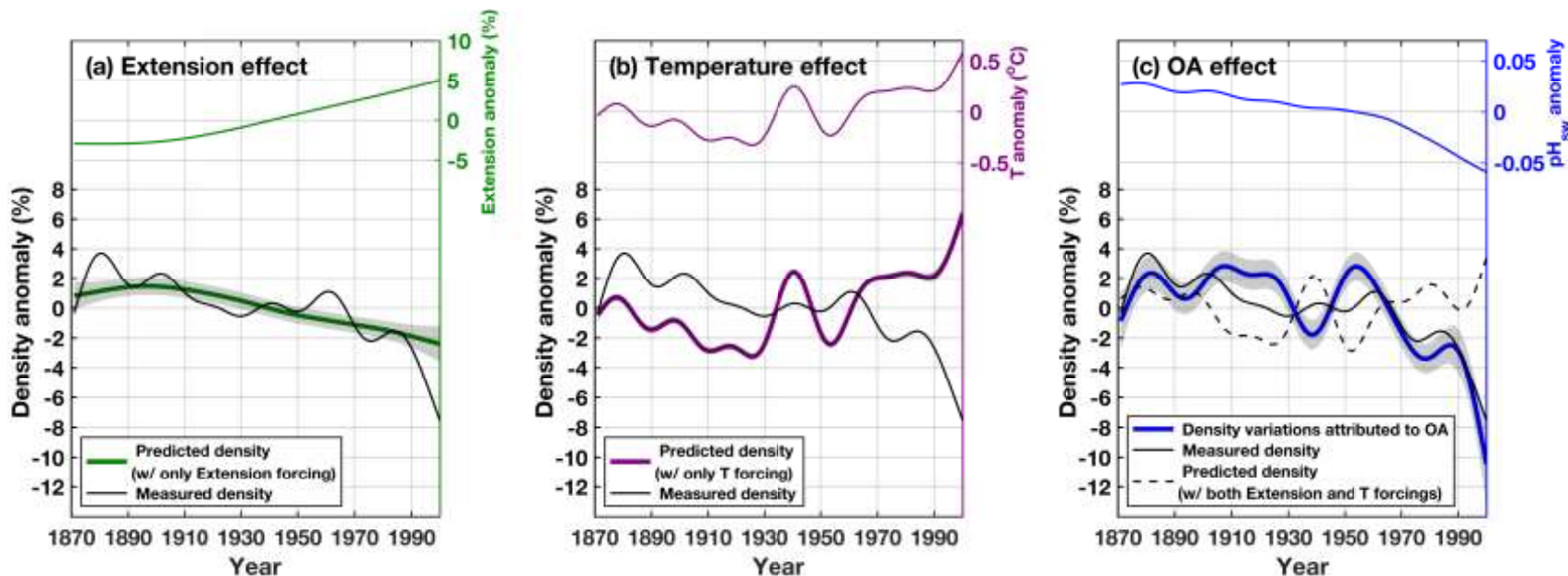
521 density indirectly through their influences on the skeletal extension and/or reef-water chemistry.

522 We use a coral skeletal growth model to isolate the effects of different factors and quantify their

523 respective contributions to the coral growth (Equation 1, Fig. 3). Arrows denote the processes

524 that are explicitly (red) or implicitly (gray) simulated in our coral skeletal growth model, and the

525 factors influencing reef water carbonate chemistry (blue).



526

527

528

529

530

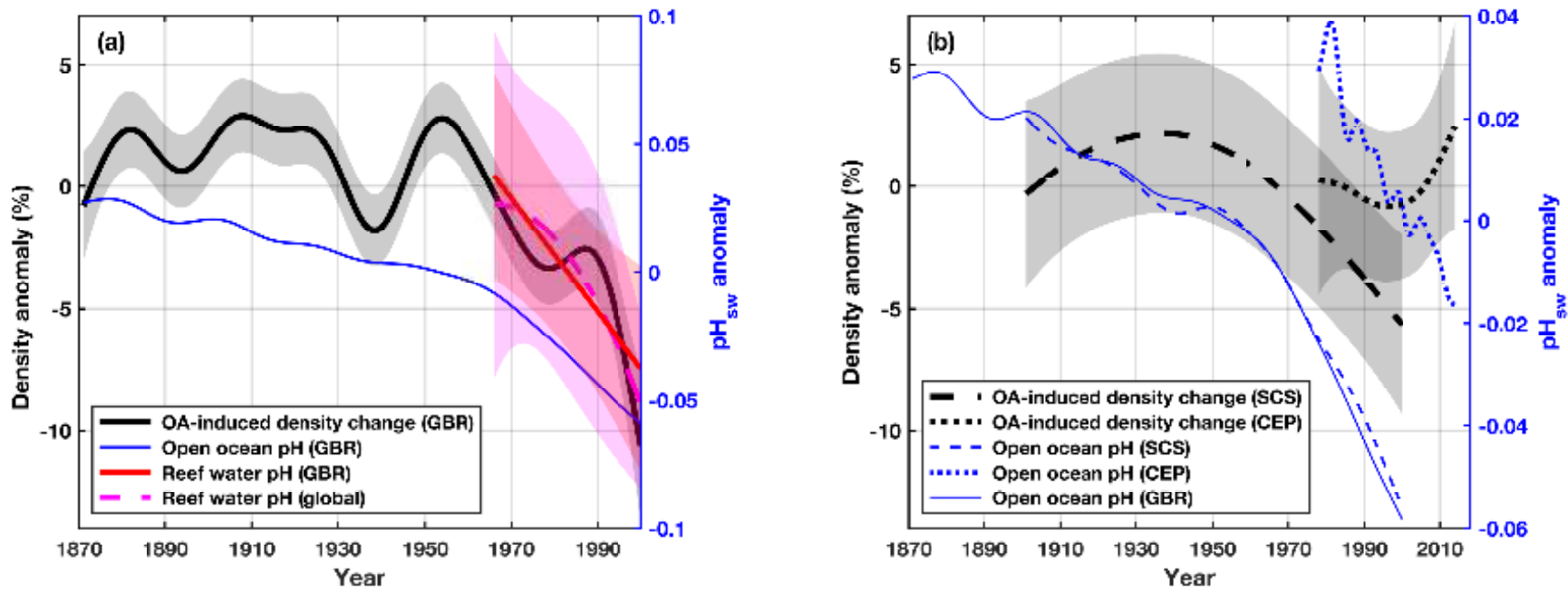
531

532

533

534

Fig. 3. Contributions of different factors to the changes in *Porites* skeletal density at the Great Barrier Reef: (a) extension, (b) temperature, and (c) ocean acidification. The impact of ocean acidification is determined by subtracting the model predicted effects of extension and temperature (dashed line, panel c) from the measured density (black line, Equation 1). Also shown for comparison are the temporal changes in each factor (upper panels). All anomalies are calculated relative to the corresponding mean values over 1951-1960, a common period that all cores cover, and the seawater temperature and pH are derived from the HadiSST dataset and the CESM-BGC historical run, respectively (Methods). The model-predicted high-frequency density variability around 1940 (b-c) likely arises from the uncertainties in the historical temperature data-products during this time period (see text for details).



535

536

537 **Fig. 4. Impacts of OA on *Porites* skeletal density at different reef systems and their correlations with ocean and reef-water pH:**

538 **(a) Great Barrier Reef (GBR), (b) South China Sea (SCS) and central equatorial Pacific (CEP) reefs.** The declines in reef-water pH at

539 the GBR (Methods, Pelejero et al., 2005; Wei et al., 2009; D'Olivo et al., 2015) and other reefs around the globe (Cyronak et al., 2014)

540 are shown in (a). Also shown for comparison are the open-ocean pH derived from the Community Earth System Model

541 Biogeochemical (CESM-BGC) historical run. The gray and colored bands indicate 95% confidence intervals.